New Cosmological Data and the Values of the Fundamental Parameters
IAU Symposium, Vol. 201, 2005
Anthony Lasenby and Althea Wilkinson, eds.

Cosmic Data Fusion

S. L. Bridle
OMP, 14 avenue E. Belin, F-31400, Toulouse, France; Cavendish Laboratory, Madingley Road, Cambridge CB3 0HE, UK

Abstract. We compare and combine likelihood functions of the cosmological parameters $\Omega_{\rm m}$, h and σ_8 from the CMB, type Ia supernovae and from probes of large scale structure. We include the recent results from the CMB experiments BOOMERANG and MAXIMA-1. Our analysis assumes a flat ΛCDM cosmology with a scale-invariant adiabatic initial power spectrum. First we consider three data sets that directly probe the mass in the Universe, without the need to relate the galaxy distribution to the underlying mass via a "biasing" relation: peculiar velocities, CMB and supernovae. We assume a baryonic fraction as inferred from Big-Bang Nucleosynthesis and find that all three data sets agree well, overlapping significantly at the 2σ level. This therefore justifies a joint analysis, in which we find a joint best fit point and 95% confidence limits of $\Omega_{\rm m} = 0.28\,(0.17, 0.39)$, $h = 0.74\,(0.64, 0.86)$, and $\sigma_8 = 1.17\,(0.98, 1.37)$. Secondly we extend our earlier work on combining CMB, supernovae, cluster number counts, IRAS galaxy redshift survey data to include BOOMERANG and MAXIMA-1 data and to allow a free $\Omega_{\rm b}h^2$. We find that, given our assumption of a scale invariant initial power spectrum ($n = 1$), we obtain the robust result of $\Omega_{\rm b}h^2 = 0.031 \pm 0.03$, which is dominated by the CMB constraint.

1. Introduction

A simultaneous analysis of the constraints placed on the cosmological parameters by various different kinds of data is essential because each different probe typically constrains a different combination of the parameters. By considering these constraints together, one can overcome any intrinsic degeneracies to estimate each fundamental parameter and its corresponding random uncertainty. The comparison of constraints can also provide a test for the validity of the assumed cosmological model or, alternatively, a revised evaluation of the systematic errors in one or all of the data sets. Recent papers that combine information from several data sets simultaneously include Gawiser & Silk (1998), Bridle et al. (1999; 2000), Bahcall et al. (1999), Bond & Jaffe (1999), Lineweaver (1998) and Lange et al. (2000).

The anisotropies in the Cosmic Microwave Background (CMB) depend on the state of the universe at the epoch of recombination, on the global geometry of space-time and on any re-ionization. Thus they provide a powerful and potentially accurate probe of the cosmological parameters (see Hu, Sugiyama and Silk 1997 for a review). With the recent release of results from a new generation of CMB experiments BOOMERANG and MAXIMA-1 have come a number of parameter estimation analyses, including those by Lange et al. (2000), Balbi et

https://doi.org/10.1017/S007418090021646X Published online by Cambridge University Press

al. (2000) and Tegmark & Zaldarriaga (2000). Constraints from the CMB are discussed in Section 2.

Galaxy motions relative to the Hubble flow arise from the gravitational forces due to mass-density fluctuations; they therefore reflect the underlying distribution of matter (both dark and luminous), and can thus provide constraints on the cosmological density parameter $\Omega_{\rm m}$ and the fluctuation amplitude parameter σ_8. The distances of type Ia supernovae (SN) can now be measured at large redshift. Thus they can provide constraints on the acceleration of the universal expansion, and the corresponding parameters $\Omega_{\rm m}$ and Ω_Λ, via a classical cosmological test based on the luminosity-redshift relation. Velocities, supernovae and CMB allow direct dynamical constraints free of assumptions regarding the "biasing" relation between the distribution of galaxies and the underlying matter density, which are unavoidable when interpreting galaxy redshift surveys. Cosmological parameter estimates are presented in Section 3 (for more details on this work see Bridle et al. 2000).

In Bridle et al. (1999) we investigated the combination of constraints from CMB data, the abundance of clusters of galaxies (Eke et al. 1998) and the IRAS 1.2 Jy redshift survey (Fisher, Scharf & Lahav 1994). These data sets were found to be in excellent agreement. In Section 4 this work is updated to include the BOOMERANG-98 and MAXIMA-1 data, and also $\Omega_{\rm b}h^2$ is included as a free parameter.

2. CMB constraints

We use the same compilation of CMB anisotropy measurements as in Bridle et al. (2000), marginalising over the 10 and 4 per cent calibration uncertainties quoted, respectively, for the BOOMERANG-98 and MAXIMA-1 results, fully taking into account the correlated nature of the calibration errors (Bridle et al., in preparation). We assume that the universe is flat ($\Omega_{\rm m}+\Omega_\Lambda=1$) with a scale invariant initial power spectrum ($n=1$), with negligible tensor contrubutions and negligible re-ionization. We obtain theoretical CMB power spectra as a function of the cosmological parameters using the CMBFAST and CAMB codes (Seljak & Zaldarriaga, 1996; Lewis, Challinor & Lasenby, 2000).

The COBE data constrain the large scale temperature fluctuations well, which converts to a strong constraint on σ_8 for given values of h and $\Omega_{\rm m}$. The CMB data indicate the position of the first acoustic peak, near $\ell\sim 200$ which corresponds to a wavenumber of $k\sim 0.03\ h\ {\rm Mpc}^{-1}$. This constrains the combination $\Omega_{\rm m}+\Omega_\Lambda$ to be roughly around unity (e.g. Efstathiou et al. 1999, Dodelson & Knox 2000, Lange et al. 2000, Balbi et al. 2000, Tegmark and Zaldarriaga 2000), consistent with the flat universe assumed in our current analysis. In fact using just BOOMERANG and COBE, Lange et al. (2000) find $\Omega_{\rm m}+\Omega_\Lambda\sim 1.1$ (Fig. 2), whereas using just MAXIMA-1 and COBE, Balbi et al. (2000) find $\Omega_{\rm m}+\Omega_\Lambda\sim 0.9$.

At $\sim 1^\circ$ angular scales the height of the first acoustic peak constrains the matter-radiation ratio at last scattering, and this ratio is proportional to $\Omega_{\rm m}h^2$. In addition, given our assumption of a flat universe, $\Omega_{\rm m}$ and h also significantly affect the position of the first acoustic peak (see Fig 2. of White, Scott and Pierpaoli 2000 for an illustration). Increasing $\Omega_{\rm m}$ moves the peak

https://doi.org/10.1017/S007418090021646X Published online by Cambridge University Press

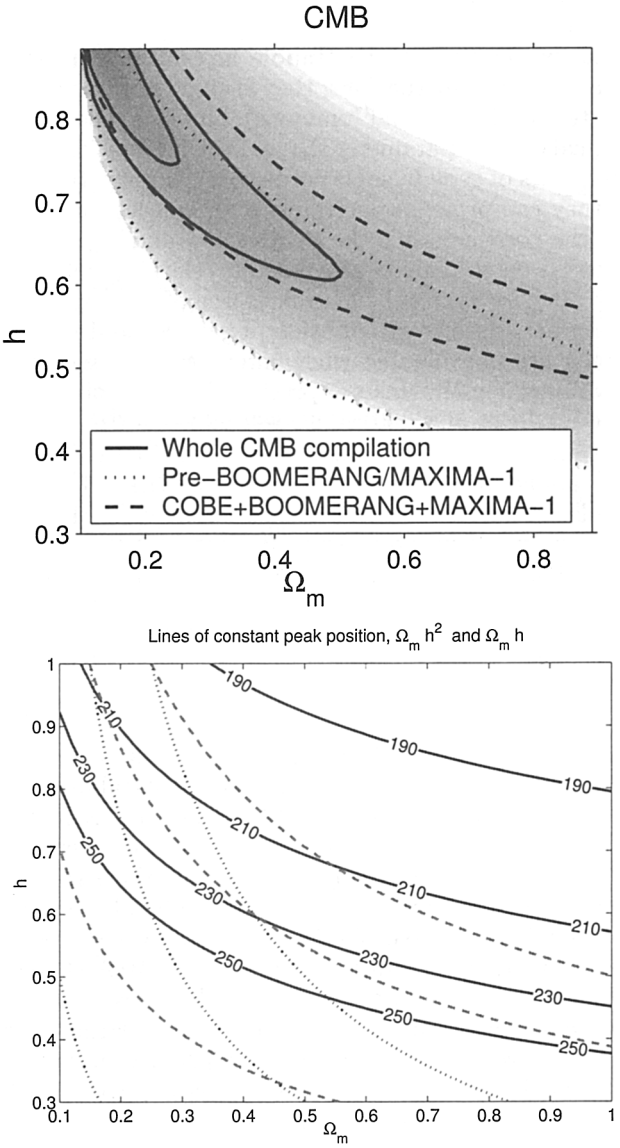

Figure 1. Top: Constraints in the $\Omega_{\rm m}$, h plane from the CMB data (marginalised over σ_8 and with $\Omega_{\rm b}h^2$ fixed at 0.019). Solid lines show the 68, 95 % limits using the whole CMB data compilation. 95 % contours from the pre-BM and from just COBE+BOOMERANG-98+MAXIMA-1 data are shown by the dotted and dashed lines respectively. Bottom: Dashed lines are at $\Omega_{\rm m}h^2 = 0.05, 0.15, 0.25$. Dotted lines are at $\Omega_{\rm m}h = 0.1, 0.2, 0.3$. Solid lines are at the peak positions labelled, given $\Omega_{\rm m} + \Omega_\Lambda = 1$, $\Omega_{\rm b}h^2 = 0.019$.

https://doi.org/10.1017/S007418090021646X Published online by Cambridge University Press

to lower ℓ, as does increasing h. These two effects combine to give the likelihood distribution in the $\Omega_{\rm m}$-h plane shown in the left hand panel of Fig. 1 (for $\Omega_{\rm b}h^2 = 0.019$). The slightly lower first peak height indicated by the BOOMERANG and MAXIMA-1 data and the lower ℓ position of the first peak from the BOOMERANG data produce a constraint at higher $\Omega_{\rm m}$ and h than does the pre-BOOMERANG/MAXIMA-1 compilation (hereafter pre-BM). Using the whole compilation together defines a region in ($\Omega_{\rm m}$,h) space at the intersection of the BOOMERANG+MAXIMA-1 and the pre-BM contours. This occurs at high h and low $\Omega_{\rm m}$. It is interesting to note that the degeneracy directions for each of the pre-BM and the BOOMERANG+MAXIMA-1 data sets are somewhat different (as shown in Fig. 1b.). One possible explanation for this is that the older data put a strong constraint on the peak height, which is a function of $\Omega_{\rm m}h^2$. On the other hand the BOOMERANG+MAXIMA-1 data, with their detailed ℓ space coverage but significant calibration uncertainties, place a strong constraint on the peak position. Lines of constant peak position lie more parallel to the $\Omega_{\rm m}$ axis than do lines of constant $\Omega_{\rm m}h^2$, shown in Fig. 1 (derived from Efstathiou and Bond 1999, discussed in more detail in Bridle 2000). Therefore using the whole CMB compilation allows tighter constraints to be placed on h and $\Omega_{\rm m}$.

Increasing $\Omega_{\rm b}h^2$ (for fixed $\Omega_{\rm m}h^2$) incraeses the first peak height while decreasing the second peak height, which improves the fit to the BOOMERANG-98 and MAXIMA-1 data, as discussed elsewhere in these proceedings. If $\Omega_{\rm b}h^2$ is changed to 0.03 from 0.019, the preferred region in the $\Omega_{\rm m}$, h plane (Fig. 1) shifts to higher $\Omega_{\rm m}$ and h (since increasing $\Omega_{\rm m}h^2$ brings the first peak height back down).

3. Comparison and Combination with Peculiar Velocities and Supernovae

We use the SFI peculiar velocity catalogue (Haynes et al. 1999a,b) which consists of $\sim$1300 spiral galaxies. The analysis follows in general the maximum-likelihood method of Zaroubi et al. (1997) and Freudling et al. (1999). Note that the linear analysis of the velocity data addresses the scaled power spectrum $P(k)\Omega_{\rm m}^{1.2}$ rather than $P(k)$ itself, and it therefore constrains the combination of parameters $\sigma_8\Omega_{\rm m}^{0.6}$, which serves as a measure of the power-spectrum amplitude. This result is almost independent of Ω_Λ (Lahav et al. 1991). In order to account for nonlinear effects acting on small scales, we add to the linear velocity correlation model an additional free parameter, $\sigma_{\rm v}$, representing an uncorrelated velocity dispersion at zero lag (this is discussed in more detail in Silberman et al., in preparation, and Bridle et al. 2000). In the absence of any other information, we have carried out the Bayesian procedure for the case where we have no knowledge of a free parameter: we have marginalised over $\sigma_{\rm v}$. The velocity data constraints at the 95% confidence level are $0.48 < \sigma_8\Omega_{\rm m}^{0.6} < 0.86$ and $0.16 < \Omega_{\rm m}h < 0.58$, with roughly uncorrelated errors.

We use the supernova Ia constraints obtained by Perlmutter et al. (1999), which are fully consistent with those of Riess et al. (1998), based on applying the classical luminosity-redshift test to distant type Ia supernovae. The sample consists of 42 high-redshift SN ($0.18 \leq z \leq 0.83$), supplemented by 18 low-

https://doi.org/10.1017/S007418090021646X Published online by Cambridge University Press

redshift SNe ($z < 0.1$). This analysis determines a combination of $\Omega_{\rm m}$ and Ω_Λ. Note that, unlike PV and CMB, SN are insensitive to the form of the matter power spectrum and depend only on the overall geometry of the universe. Since we limit ourselves in this paper to a flat universe, the SN constraint is translated to a likelihood function of $\Omega_{\rm m}$, roughly $0.13 < \Omega_{\rm m} < 0.44$.

In order to examine how well the constraints from PV, CMB and SN agree with each other we plot in Fig. 2 the three corresponding iso-likelihood surfaces, at the 2-sigma level, in the three-dimensional parameter space $(h, \sigma_8, \Omega_{\rm m})$. The upper and lower 95 per cent limits on $\Omega_{\rm m}$ from SN are the two horizontal planes. The PV surface encloses a space at roughly constant $\Omega_{\rm m}h$ and $\sigma_8\Omega_{\rm m}^{0.6}$. The CMB surface lies in the intersection of the regions allowed by each of SN and PV. The fact that the constraints have a common region of overlap is not trivial; it indicates a reasonable goodness of fit between the three data sets within the framework of the assumed cosmological model, which justifies a joint likelihood analysis aimed at parameter estimation. To illustrate the complementary nature of these three data sets and for comparison the result of using the pre-BM CMB data instead is shown in the bottom left panel of Fig. 2.

The best fit cosmological parameters given all three data sets are $h = 0.74$, $\Omega_{\rm m} = 0.28$ and $\sigma_8 = 1.17$, from which we can derive $\sigma_8\Omega_{\rm m}^{0.6} = 0.54$, $\Omega_{\rm m}h = 0.21$, $Q_{\rm rms-ps} = 19.7\mu$K and the age of the universe is 13.2 Gyr. We may evaluate the probability of a single cosmological parameter, independent of the values of the other cosmological parameters, by integrating the probability over the values of the other parameters. This is what we mean by 'marginalisation'. The solid lines in Fig. 3 shows the resulting 1-dimensional marginalised likelihood distributions for each parameter. We obtain the 95 per cent limits by integrating the one- dimensional likelihood distributions and requiring that 95 per cent of the probability lies between the quoted limits: $0.64 < h < 0.86$, $0.17 < \Omega_{\rm m} < 0.39$, $0.98 < \sigma_8 < 1.37$ The h range agrees well with that from the HST key project of $h = 0.72 \pm 0.08$ ($1-\sigma$, Freedman et al. 2000) and the $\Omega_{\rm m}$ limits are roughly centered on the popular value of 0.3.

We have repeated the entire analysis using different subsets of CMB data. Using the pre-BM data the 1-dimensional marginalised likelihood functions (dotted lines in Fig. 3) are in good agreement but somewhat wider than when using all the data, especially in the constraint on h which extends to lower values than before. Using just the COBE, BOOMERANG-98 and MAXIMA-1 data (dashed lines) the results are very similar to when all data is used. At first this may seem surprising given the much larger 3-dimensional surface, but the high $\Omega_{\rm m}$, h part is ruled out by both PV and SN, leaving virtually the same region as when all CMB data are used.

In the region of the power spectrum where a second acoustic peak is predicted, we note that our best fitting models are not a good fit to the data, producing more power than observed by both BOOMERANG and MAXIMA-1 (see for example the power spectra plotted in Bridle et al. 2000).

4. Constraints on the Baryon Density

In this section we allow the baryon density, $\Omega_{\rm b}h^2$, to vary as a free parameter, along with $\Omega_{\rm m}$, h and σ_8. We investigate combining the CMB and su-

https://doi.org/10.1017/S007418090021646X Published online by Cambridge University Press

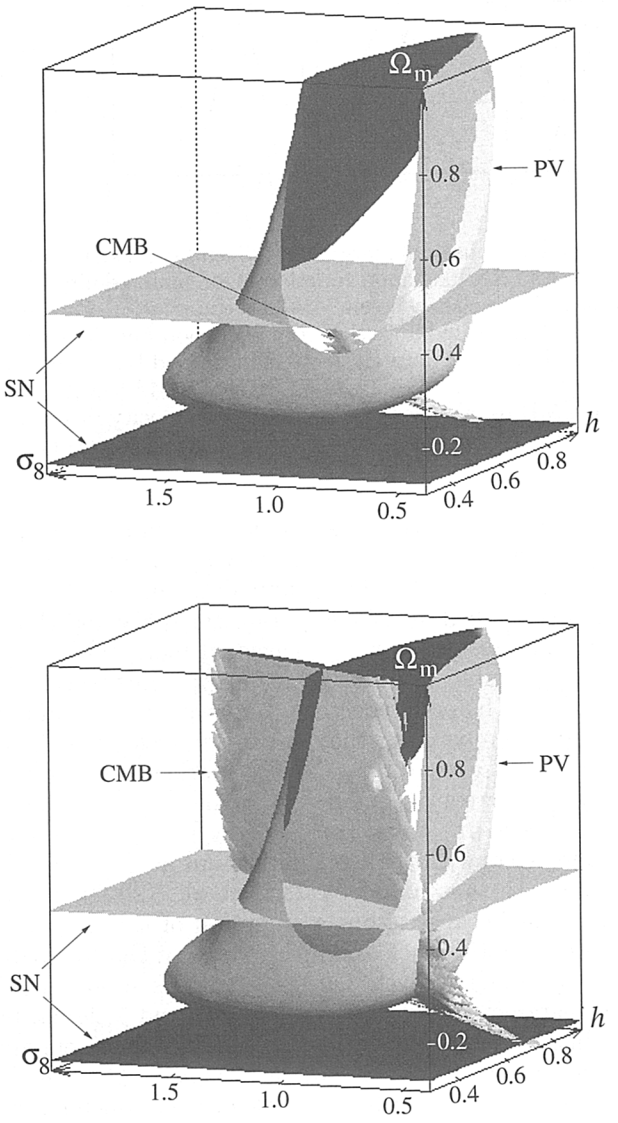

Figure 2. Top: PV, CMB (whole compilation) and SN 2σ iso-probability surfaces. For PV and CMB the surfaces are at $\Delta\log(\text{Likelihood})=4.01$, and for the SN the surfaces are at $\Delta\log(\text{Likelihood})=2.00$, corresponding to the 95 per cent limits for 3 and 1 dimensional Gaussian distributions respectively. The SN surfaces are two horizontal planes. Bottom: the same but this time the data used for the CMB surface is the pre-BM data.

https://doi.org/10.1017/S007418090021646X Published online by Cambridge University Press

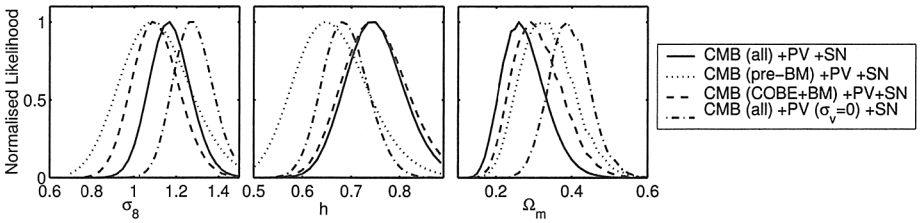

Figure 3. The 1-dimensional marginalised likelihood distributions from the joint PV, CMB and SN likelihood function. Our main results are shown by the solid lines, which use the whole CMB data compilation, PV (marginalised over σ_v) and SN. The dotted lines show the likelihood functions when PV, SN and just the pre-BM CMB data are used. The dashed line is the result when the CMB data is just COBE + BOOMERANG + MAXIMA-1. The result (using all the CMB data) when the uncorrelated velocity dispersion term is not included in the PV analysis ($\sigma_v = 0$) is shown by the dot-dashed line.

pernova data used above with the galaxy cluster number count data of Eke et al. (1998) and the IRAS galaxy redshift survey spherical harmonic analysis of Fisher, Scharf and Lahav (1994). These four data sets are found to enclose a common volume in the four dimensional parameter space and thus a joint analysis is reasonable. The resulting one-dimensional marginalised constraints are shown in Fig. 4. The h value is similar to in the previous section. The σ_8 value is somewhat lower than before, reflecting the lower $\sigma_8\Omega_m^{0.6}$ value preferred by cluster number counts compared to that found from velocities. The Ω_m value is now lower than before, at around 0.2, which is suprising given our comments at the end of Section 2. However a detailed examination in the four dimensional space reveals that this is due to the precise way in which the cluster number count constraint intersects with the CMB constraint at these high h values. The $\Omega_b h^2$ value is similar to that found by Jaffe et al. (2000) (see also Bond in these proceedings), but because of our assumption of $n = 1$, the error bars are much smaller, ruling out the nucleosynthesis value of $\Omega_b h^2 = 0.019$ (Burles et al. 1999) at the 3 to 4 sigma level. On using various subsets of the data, the constraints on all parameters but $\Omega_b h^2$ vary by around 1 sigma, but this $\Omega_b h^2$ result remains robust. This is due to the fact that all data sets apart from the CMB are relatively insensitive to the value of $\Omega_b h^2$. Also the $\Omega_b h^2$ value is not too strongly coupled to the other cosmological parameters, relative to the tightness of the CMB constraint.

5. Conclusion

The addition of BOOMERANG and MAXIMA-1 to our CMB data compilation brought down the height of the first acoustic peak and shifted it to larger angular scales, which both increase a combination of h and Ω_m. The combination of BOOMERANG and MAXIMA-1 with the older CMB data had the effect of

https://doi.org/10.1017/S007418090021646X Published online by Cambridge University Press

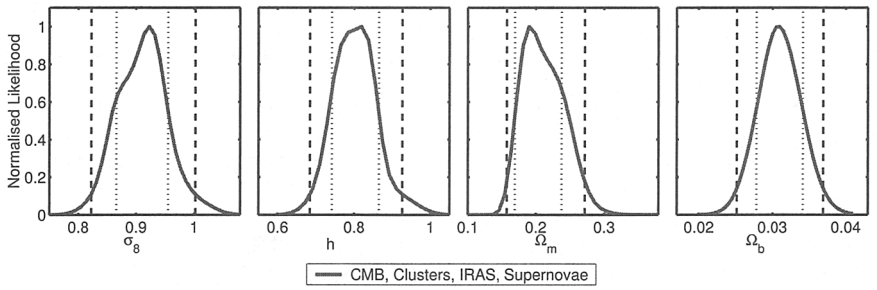

Figure 4. The 1-dimensional marginalised likelihood distributions from the joint CMB, SN, cluster and IRAS likelihood function.

breaking the degeneracy between h and Ω_m and leaving a high h region of parameter space.

We have performed a joint analysis of three complementary data sets free of galaxy-density biasing, using peculiar velocities, CMB anisotropies, and high-redshift supernovae. The constraints from the three data sets overlap well at the 2-sigma level and there is acceptable goodness of fit. These data sets constrain roughly orthogonal combinations of the cosmological parameters, and are combined to provide tighter constraints on the parameters. The values obtained from the joint analysis for h and $\Omega_{\rm m}$, and for the combinations of cosmological parameters, are in general agreement with other estimates (eg. Bahcall et al. 1999), but this analysis tends to favor a slightly higher value for σ_8. The resulting constraint on the Hubble constant, $h = 0.75 \pm 0.11$ (95 per cent confidence), agrees well with that from the HST key project value of $h = 0.72 \pm 0.08$. This result is also similar to that of Lange et al. (2000, Table 1, P10).

Motivated by the low second peak height implied by the BOOMERANG-98 and MAXIMA-1 results, we consider the effect of including $\Omega_{\rm b}h^2$ as a free parameter. Our result for $\Omega_{\rm b}h^2$ is robust at a similar value to that found by other authors (including Jaffe et al. 2000 and Bond in these proceedings), but because we have assumed a scale invariant initial power spectrum, our error bars are approximately half the size.

Note that in this analysis we take all the data sets used at equal weight. An extension to this work would be to allow freedom in the weights given to the different probes, as discussed by Lahav in this proceedings and in Lahav et al. (2000).

Acknowledgments. I thank my collaborators, O. Lahav, A. Lasenby, M. Hobson, I. Zehavi, A. Dekel, C. Frenk, V. Eke, J. P. Henry, S. Cole for their contribution. I also thank G. Rocha for her work on compilation of the CMB data set, G. Efstathiou for providing the supernova likelihoods and the referee of work included here, S. Zaroubi.

References

Bahcall, N., Ostriker, J., Perlmutter, S. & Steinhardt, P. 1999, Science, 284, 1481
Balbi et al. 2000, ApJ, submitted (astro-ph/0005124)
Bond, J. R. & Jaffe, A. H. 1998 Philosophical Transactions of the Royal Society of London A, 1998. "Discussion Meeting on Large Scale Structure in the Universe," Royal Society, London, March 1998.
Bridle, S. L., Eke, V. R., Lahav, O., Lasenby, A. N., Hobson, M. P., Cole, S., Frenk, C. F. & Henry, J. P. 1999, MNRAS, 310, 565
Bridle, S. L., Zehavi, I., Dekel, A., Lahav, O., Hobson, M. P. & Lasenby, A. N. 2000, MNRAS, in press (astro-ph/0006170)
Burles, S., Nollett, K. M., Truran, J. N. & Turner, M. S. 1999, Phys.Rev.Lett., 82, 4176
Dodelson, S. & Knox, L. 2000, Phys.Rev.Lett., 84, 3523
Efstathiou, G., Bridle, S. L., Lasenby, A. N., Hobson, M. P. & Ellis, R. S. 1999, MNRAS, 303, L47
Efstathiou, G. & Bond, J. R. 1999, MNRAS, 304, 75
Efstathiou, G., Bond, J. R. & White, S. D. M. 1992, MNRAS, 258, 1
Eke, V. R., Cole, S., Frenk, C. S. & Henry, J. P. 1998, MNRAS, 298, 1145
Fisher, K. B., Scharf, C. A. & Lahav, O. 1994, MNRAS, 266, 219
Freedman, W. L. et al. 2000, ApJ, in press (astro-ph/0012376)
Freudling et al. 1999, ApJ, 523, 1
Gawiser E. & Silk J., 1998, Science, 280, 1405
Haynes, M. P., Giovanelli, R., Salzer, J. J., Wegner, G., Freudling, W., da Costa, L. N., Herter, T. & Vogt, N. P. 1999a, AJ, 117, 1668
Haynes, M. P., Giovanelli, R., Chamaraux, P., da Costa, L. N., Freudling, W., Salzer, J. J. & Wegner, G. 1999b, AJ, 117, 2039
Hu, W., Sugiyama, N. & Silk, J. 1997, Nature 386, 6
Jaffe, A. et al. 2000, submitted to PRL (astro-ph/0007333)
Lahav, O., Bridle, S. L, Hobson, M. P., Lasenby, A. N. & Sodre Jr., L. 1999, MNRAS, 315, 45L
Lange, A. E. et al. 2000, preprint (astro-ph/0005004)
Lewis, A., Challinor, A. & Lasenby, A. 2000, ApJ, in press (astro-ph/9911177)
Lineweaver, C. H. 1998, ApJ, 505, L69
Perlmutter, S. et al. 1999, ApJ, 517, 565
Riess, A. G. et al. 1998, AJ, 116, 1009
Seljak, U. & Zaldarriaga, M. 1996, ApJ, 469, 437
Tegmark, M. & Zaldarriaga, M. 2000, preprint (astro-ph/0004393)
Zaroubi, S., Zehavi, I., Dekel, A., Hoffman, Y. & Kolatt, T. 1997, ApJ, 486,